Published OnlineFirst July 28, 2009; DOI: 10.1158/0008-5472.CAN-08-4721



# Follicle-Stimulating Hormone Peptide Can Facilitate Paclitaxel Nanoparticles to Target Ovarian Carcinoma *In vivo*

Xiao-yan Zhang,[1] Jun Chen,[2] Yu-fang Zheng,[4] Xiao-ling Gao,[7] Yu Kang,[1] Jia-chi Liu,[3] Ming-jun Cheng,[1] Hong Sun,[1] and Cong-jian Xu[1,5,6]

[1]Obstetrics and Gynecology Hospital, Departments of [2]Pharmaceutics and [3]Pharmaceutical Analysis, School of Pharmacy, [4]School of Life Sciences, [5]Department of Obstetrics and Gynecology of Shanghai Medical School, and [6]Institutes of Biomedical Sciences, Fudan University; [7]Department of Pharmacology, Institute of Medical Sciences, Shanghai Jiaotong University School of Medicine, Shanghai, People's Republic of China

## Abstract

**Chemotherapy is an important treatment for ovarian cancer. However, conventional chemotherapy has inevitable drawbacks due to side effects from nonspecific biodistribution of the chemotherapeutic drugs. To solve such problem, targeted delivery approaches were developed. The targeted delivery approaches combine drug carriers with the targeting system and can preferentially bring drugs to the targeted sites. Follicle-stimulating hormone receptor (FSHR) is an ovarian cancer–specific receptor. By using a peptide derived from FSH (amino acids 33–53 of the FSH β chain, named as FSH33), we developed a conjugated nanoparticle, FSH33-NP, to target FSHR in ovarian cancer. FSH33-NP was tested for recognition specificity and uptake efficiency on FSHR-expressing cells. Then, the antitumor efficiency of paclitaxel (PTX)-loaded FSH33-NP (FSH33-NP-PTX) was determined. FSH33-NP-PTX displayed stronger antiproliferation and antitumor effects compared with free PTX or naked PTX-loaded nanoparticles (NP-PTX) both *in vitro* and *in vivo*. In summary, this novel FSH33-NP delivery system showed very high selectivity and efficacy for FSHR-expressing tumor tissues. Therefore, it has good potential to become a new therapeutic approach for patients with ovarian cancer.** [Cancer Res 2009;69(16):6506–14]

## Introduction

Ovarian cancer is the leading cause of gynecologic malignancies. Because it often has no typical symptoms in the early stages, most patients are diagnosed at advanced stages and have only a 30% 5-year survival rate.[8] The routine treatment for patients with advanced-stage disease is a combination of cytoreductive surgery and chemotherapy. However, conventional chemotherapy has inevitable drawbacks because of the side effects from nonspecific biodistribution of the chemotherapeutic drugs (1). Thus, research on targeted drug delivery system has focused on how to improve efficiency and reduce the side effects at the same time. Unmodified nanoparticles have been used as drug carriers to ensure more efficient drug delivery (2). However, a majority of the drugs they carry will concentrate in the liver and spleen through the circulation, not the targeted foci. On the other hand, active drug-targeting systems could avoid such downside as they have modified drug-delivering microparticles based on the specific binding of certain modified small molecules to targeted cells, ensuring specific drug delivery into the targeted sites (3–5). The combination of active targeting system and nanoparticulate carriers might be a promising approach, which can not only target specifically to tumor foci but also load more drugs to those sites (6).

An important step for the new system is to modify drug carriers and conjugate drug molecules to nanoparticles. Poly(lactic acid) (PLA) nanoparticles are a good choice for such a modification based on their chemical characters (7, 8). The surface modifications of polyethylene glycol (PEG) and methoxy-PEG (MPEG) could enable PLA nanoparticles to escape uptake by the mononuclear phagocytic system so as to prolong its blood half-life (9–12). The maleimide groups on maleimide-PEG-PLA make it possible for nanoparticles to covalently couple to molecules with sulfhydryl groups, such as antibodies or peptides (11, 13, 14), which bind to specific cell surface receptors and mediate endocytosis after binding.

Therefore, the choice of conjugated antibody or peptide as target-specific ligand is also important for specific therapeutic purposes. The ovary is the target organ of follicle-stimulating hormones (FSH), which bind to the FSH receptor (FSHR), a G protein–linked receptor. FSHR was found in the ovarian surface epithelium (OSE) and in some ovarian cancer cell lines and tissues (15–21); however, its distribution may be limited in the reproductive system (22). This expression pattern makes it possible to use FSHR as the target site against ovarian cancer. FSH is a glycoprotein hormone consisting of α and β chains, and some FSHR-binding domains have been identified, including amino acids 1 to 15, 33 to 53, 51 to 65, and 81 to 95 of the FSH β chain (23–26). Because FSH β 33-53 has the strongest binding affinity (data not shown; ref. 24), it is used in our system as a target-specific ligand to distribute drugs to ovarian tumor tissue.

In our study, we investigated the potential of FSH β 33-53 peptide–conjugated PEG-PLA nanoparticles (FSH33-NP) as a novel drug delivery system. First, the expression of FSHR was examined in human ovarian cancer cell lines and tissue specimens. Then, the recognition specificity and uptake efficiency of FSH β 33-53 peptide and FSH33-NP were evaluated by fluorescent probes. A chemotherapeutic drug, paclitaxel (PTX), was chosen as a model drug to test our delivery system. The antitumor effect of PTX-loaded nanoparticles (NP-PTX) against ovarian cancer was studied both

**Note:** Supplementary data for this article are available at Cancer Research Online (http://cancerres.aacrjournals.org/).

X-y. Zhang and J. Chen contributed equally to this work.

**Requests for reprints:** Cong-jian Xu, Obstetrics and Gynecology Hospital, Fudan University, 419 Fangxie Road, Shanghai 200011, People's Republic of China. Phone: 86-21-6345-5050; Fax: 86-21-6345-0944; E-mail: xucongjian@gmail.com.



doi:10.1158/0008-5472.CAN-08-4721

[8] Ries LAG, Melbert D, Krapcho M, et al. SEER cancer statistics review, 1975-2005, National Cancer Institute. Bethesda, MD, http://seer.cancer.gov/csr/1975_2005/, based on November 2007 SEER data submission, posted to the SEER Web site, 2008.

Published OnlineFirst July 28, 2009; DOI: 10.1158/0008-5472.CAN-08-4721



*in vitro* and *in vivo*, and our results indicated that PTX-loaded FSH33-NP (FSH33-NP-PTX) has a better therapeutic effect against ovarian cancer compared with NP-PTX or PTX alone.

## Materials and Methods

**Materials.** MPEG was obtained from NOF Corp. and maleimide-PEG was from Nektar. D,L-lactide was from Purac, and coumarin 6 was from Sigma. PTX was purchased from Xi'an Sanjiang Bio-Engineering, and commercial PTX injection was from Hualian Pharmaceutical Factory. Rabbit anti-human/mouse/rat FSHR polyclonal antibody was from Santa Cruz Biotechnology.

Tissues of 30 human ovarian carcinoma specimens were obtained from patients (ages 51.60 ± 10.03 y; 23–72 y) admitted at the Obstetrics and Gynecology Hospital of Fudan University after informed consent was given. All specimens were identified by two pathologists following a double-blind test.

Human ovarian carcinoma cell line Caov-3 was obtained from the Reproductive Health Laboratory of the Women's Hospital, Zhejiang University (Hangzhou, China). Human ovarian carcinoma cell lines ES-2, OVCAR-3, and SKOV-3 were purchased from the Cell Bank of the Chinese Academy of Science (Shanghai, China). Normal OSE cells were collected and cultured with informed consent from the donors according to the protocol of the University of Texas M. D. Anderson Cancer Center.

Female BALB/c mice (Shanghai Cancer Institute, Shanghai, China) used in this study were treated according to the protocols approved by the ethical committee of Fudan University.

**Preparation of FSH33-NP.** Peptide FSH β 33-53 (YTRDLVYKDPARP-KIQKTCTF) was synthesized and purified by high-performance liquid chromatography (HPLC). Nanoparticles were prepared with maleimide-PEG-PLA and MPEG-PLA, which were synthesized by ring opening polymerization (11, 27), using the emulsion/solvent evaporation technique (28). Maleimide-PEG-PLA and MPEG-PLA were dissolved in dichloromethane and emulsified by sonication. Another emulsification was done in 2 mL of 1% sodium cholate aqueous solution. The water-oil-water multiple emulsions were diluted into 25 mL of 0.5% sodium cholate aqueous solution. After evaporation at 40°C, the nanoparticles were collected by centrifugation. Coumarin 6–loaded nanoparticles were prepared in the same way, except that coumarin 6 was added to the copolymer solution before primary emulsification.

NP-PTX was prepared by an oil-water emulsification solvent evaporation method (29). PTX (5 mg) was dissolved in 4 mL of dichloromethane containing 2.5% maleimide-PEG-PLA and MPEG-PLA. The organic phase was then added into 20 mL of 1% sodium cholate aqueous solution and sonicated. The resulting emulsion was stirred at 40°C to evaporate dichloromethane. The nanoparticles were collected by centrifugation.

To prepare FSH33-NP, the mixture of FSH β 33-53 peptide and nanoparticles (the molar ratio of FSH β 33-53 peptide and maleimide was 1:1) was magnetically stirred overnight. The reaction mixture was then isolated on a Sepharose CL-4B column by elution with HEPES buffer. The milky FSH33-NP fractions were collected.

**Nanoparticle characterization.** The morphology of nanoparticles was examined by transmission electron microscope (H-600; Hitachi). The diameter and ζ potential were determined by dynamic light scattering analysis using Zeta Potential/Particle Sizer Nicomp 380 ZLS.

To determine the content of PTX, nanoparticles were dissolved in methanol and analyzed by a HPLC system. Optimization and validation of the HPLC method were performed (data not shown). The entrapping efficiency (EE) of PTX was calculated with the following equation:

$$\mathrm{EE}(\%) = \frac{\text{Amount of PTX in the nanoparticles}}{\text{Total amount of PTX added}} \times 100\%$$

The release of PTX from nanoparticles was examined by incubating 1 mL of NP-PTX in a dialysis bag and immersing in 100 mL of PBS (pH 7.4). The entire system was stirred at 75 rpm at 37°C. The amount of PTX released in each time interval was analyzed with the HPLC method.

To analyze the surface atomic composition of C, O, and N of nanoparticles and prove the existence of peptides on the surface of the nanoparticles, X-ray photoelectron spectroscopy (XPS) was performed using a PHI-5000C ESCA system (Perkin-Elmer). The X-ray anode was run at 250 W and the voltage was kept at 14.0 kV. The pass energy was fixed at 23.50, 46.95, or 93.90 eV. The whole spectra and narrow spectra were recorded by RBD 147 interface through AugerScan 3.21 software. Binding energies were calibrated using the containment carbon (C1s, 284.60 eV). The data were analyzed by XPS Peak Version 4.1 software.

**Immunohistochemistry and immunocytochemistry.** After deparaffinization and rehydration, the tissue sections of human ovarian cancer were incubated with FSHR antibody and then with peroxidase-conjugated anti-rabbit IgG. Control was performed with nonimmune rabbit serum. The staining reaction was done with diaminobenzadine and hematoxylin. For immunocytochemistry, cells were fixed with 4% paraformaldehyde. The remaining procedures were done in the same way.

**Xenografts and Western blot analysis.** To investigate the expression of FSHR in tumor xenografts and main organs of mice, a total of $4 \times 10^6$ SKOV-3 or Caov-3 cells were injected s.c. into the axilla of 6-wk-old female BALB/c mice. After 2 wk, tumor xenografts and the main organs of the mice were harvested. The protein extracts were separated by SDS-PAGE and transferred to nitrocellulose membranes. The membranes were incubated with FSHR antibody and β-actin antibody. After incubating with peroxidase-conjugated anti-rabbit IgG, immunodetection was performed with enhanced chemiluminescence and exposed to X-ray films.

**Peptide binding assay.** To prove whether FSH β 33-53 peptide conjugated specifically to FSHR-positive ovarian cancer cells, SKOV-3 and Caov-3 cells were incubated in PBS with 10 to 80 μmol/L of FITC-labeled FSH β 33-53 peptide for 15 to 120 min. Then, cells were rinsed with PBS and fixed with 4% paraformaldehyde. After mounting, cells were examined by fluorescence microscope (Olympus). For flow cytometry, SKOV-3 and Caov-3 cells were incubated in PBS with 20 μmol/L of FITC-labeled FSH β 33-53 peptide for 60 min. Then, cells were rinsed, collected, and analyzed.

**Cellular uptake of FSH33-NP.** To evaluate the capacity of FSH33-NP for drug delivery into FSHR-positive ovarian cancer cells, coumarin 6 was incorporated into the nanoparticles, and its concentration was detected by fluorescence microscopy and flow cytometry. The procedures were the same as before, except that cells were incubated in Hank's buffer with 0.1 to 100 μg/mL of coumarin 6–loaded nanoparticles.

**Cytotoxicity assay.** To investigate the cytotoxicity of FSH33-NP-PTX, 3-(4,5-dimethylthiazol-2-yl)-2,5-diphenyltetrazolium bromide (MTT) assay was used. Cells were incubated in serum-free medium with different concentrations (0.001–10 μmol/L) of PTX, NP-PTX, or FSH33-NP-PTX for 6 to 96 h, respectively. At the indicated times, the medium was replaced with 100 μL of MTT solutions (0.5 mg/mL). The formazan grains were dissolved in DMSO and measured by a microplate reader at 490-nm wavelength. The inhibitive rate was calculated as follows: 1 subtracts the percentage of absorbance of the study group over the control group.

**Antitumor effects of FSH33-NP-PTX *in vivo*.** To evaluate the efficient antitumor effects of FSH33-NP-PTX *in vivo*, BALB/c mice bearing human ovarian carcinoma Caov-3 xenografts were established. Twenty-eight mice were randomly divided into four groups administrated with saline, commercial PTX, NP-PTX, or FSH33-NP-PTX via tail vein at a dose of 6 mg/kg body weight, respectively. The injection was repeated every 3 d for five consecutive injections. Tumor size was measured with calipers every 2 d. Tumor volume was calculated using the following formula: $\pi/6 \times$ larger diameter $\times$ (smaller diameter)$^2$.

**Statistical analysis.** Statistical evaluations of data were performed by unpaired Student's $t$ test and one-way ANOVA. Data were expressed as mean ± SD. $P < 0.05$ was considered significant.

## Results

**Characterization of nanoparticles and covalent coupling of FSH β 33-53 peptide to the nanoparticles.** FSH β 33-53 and FITC-FSH β 33-53 were synthesized and checked for molecular weights

Published OnlineFirst July 28, 2009; DOI: 10.1158/0008-5472.CAN-08-4721



by mass spectrometry (Supplementary Fig. S1). After modification of nanoparticles, we examined the shape and size of these nanoparticles under a transmission electron microscope (Fig. 1*A*). Most nanoparticles and FSH33-NP loaded with or without coumarin 6 or PTX were spherical and had a regular size. The average diameters of nanoparticle and FSH33-NP loaded with or without coumarin 6 were all 100 nm or so (Supplementary Table S1). A diameter decrease to 51 to 78 nm was observed in NP-PTX and FSH33-NP-PTX due to the synthesis technique. The average ζ potential of all nanoparticles was −18 to −30 mV at pH 7.0, suggesting that the conjugated peptide FSH β 33-53 did not cause a notable change of ζ potential. The EE of NP-PTX was 69.33 ± 5.13%. The *in vitro* release of PTX from nanoparticles exhibited a biphasic pattern, which was characterized by a fast initial release within the first 24 hours followed by a slower and continuous release (Fig. 1*B*).

The surface chemical compositions of nanoparticles were investigated by XPS analysis. As shown in Fig. 1*C*, peaks 1 to 4 were in the C1s envelope. Peak 1 represented the carbon in C–C or C–H. Peak 2 represented the carbon in OñC–NH. Peaks 3 and 4 corresponded to the carbons of ester and carboxylate, respectively. Peaks 6 and 7 were in the O1s envelope. Peak 6 corresponded to

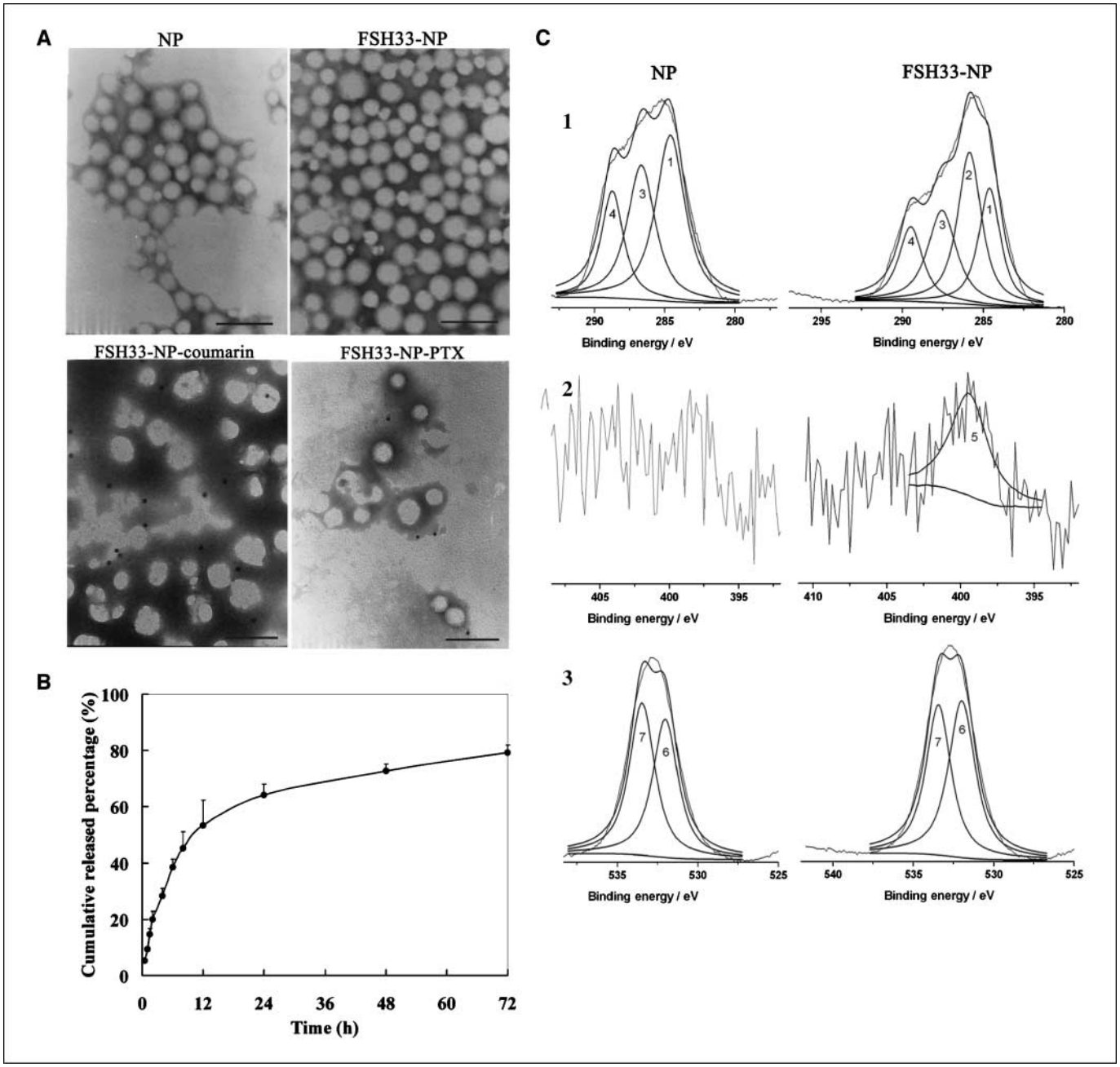


**Figure 1.** Characterization of nanoparticles. *A,* transmission electron micrographs. Nanoparticles were negatively stained with phosphotungstic acid solution. *Bar,* 100 nm. *B,* cumulative release of PTX from NP-PTX. Release was studied in PBS buffer (pH 7.4) at 37°C. *C,* carbon C1s, nitrogen N1s, and oxygen O1s envelopes of nanoparticle and FSH33-NP by XPS analysis. *1,* C1s envelope; *2,* N1s envelope; *3,* O1s envelope.

Published OnlineFirst July 28, 2009; DOI: 10.1158/0008-5472.CAN-08-4721



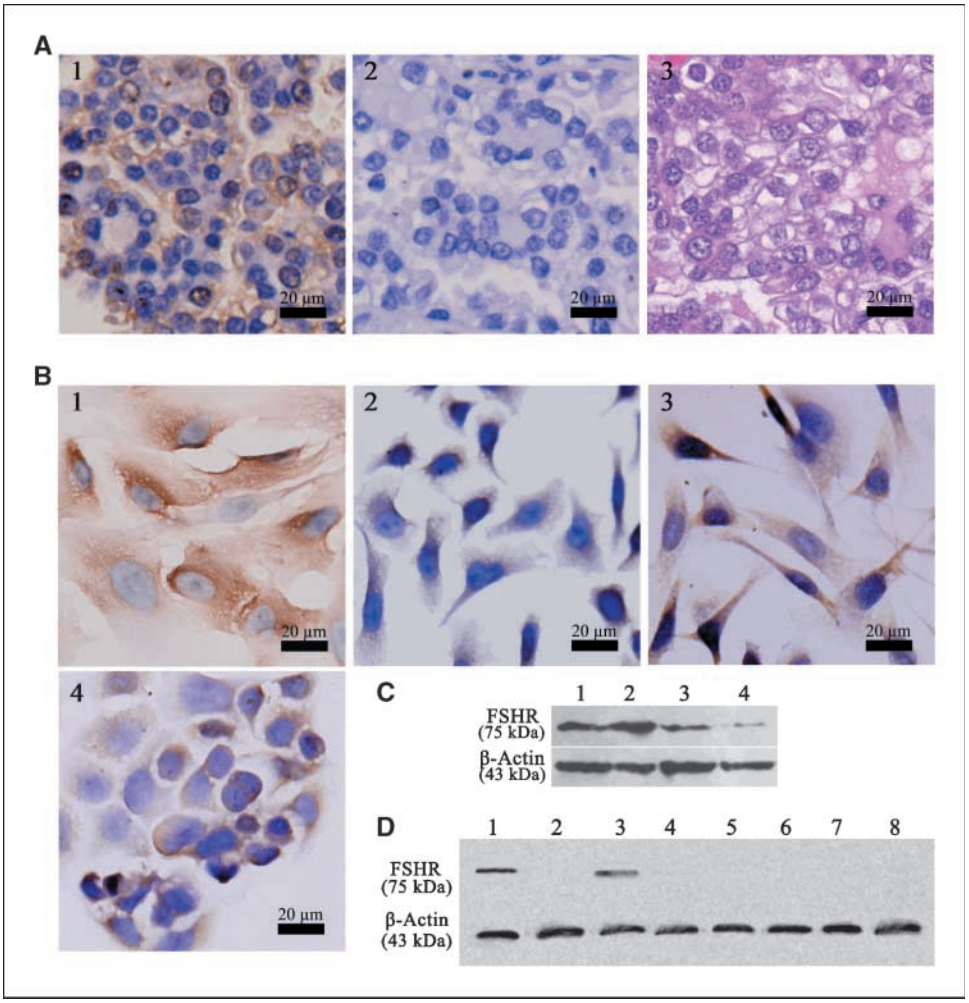


**Figure 2.** Expression of FSHR protein on human ovarian carcinoma tissue and cells. *A,* FSHR expression in human ovarian carcinoma tissues, staining with FSHR antibody (*1*) and control IgG (*2*). *3,* H&E staining. *Bar,* 20 μm. *B,* FSHR expression in different cells by immunocytochemistry. *1,* OSE cells; *2,* SKOV-3 cells; *3,* Caov-3 cells; *4,* OVCAR-3 cells. *Bar,* 20 μm. *C,* FSHR expression in different cells by Western blot. *1,* OSE cells; *2,* Caov-3 cells; *3,* ES-2 cells; *4,* OVCAR-3 cells. *D,* FSHR expression in tumor xenografts and main organs of BALB/c mice bearing human ovarian carcinoma. *1,* Caov-3 tumor; *2,* SKOV-3 tumor; *3,* uterus and ovary; *4,* heart; *5,* liver; *6,* spleen; *7,* lung; *8,* kidney.

the oxygen of OñC, and peak 7 corresponded to the oxygen of O–C. Peak 5 represented the N1s envelope.

Peak 2 of FSH33-NP was generated by OñC–NH due to covalent binding of FSH β 33-53 and the maleimide group. According to the chemical structure of nanoparticles, the nitrogen was derived from either the maleimide group or FSH β 33-53. There was no N1s envelope detected in nanoparticle, indicating that the amount of nitrogen in the maleimide group was lower than the detection limit of XPS and can be neglected (13, 30). The N1s envelope of FSH33-NP (peak 5) could be attributed to FSH β 33-53 on the surface of the nanoparticles. The percentage compositions of samples were also analyzed. The surface nitrogen was only detected in FSH33-NP with a value at 0.37% (Supplementary Table S2). This proved that the peptide covalently bound on the surface of nanoparticles.

**Expression of FSHR protein.** To evaluate the possibility of using FSHR as a therapeutic target, we first examined FSHR expression on human ovarian cancer. FSHR expression was not detected in six metastatic ovarian cancer specimens in which tumors originated from other organs, whereas a majority of the primary ovarian carcinomas (17 of 24, 70.83%) showed positive staining for FSHR (Fig. 2*A*). This high expression rate indicated that FSHR could be used as the target in our system. We also checked FSHR expression on normal ovarian epithelial cells and several human ovarian cancer cell lines. OSE, Caov-3, and ES-2 cells have higher FSHR expression levels than OVCAR-3 cells. No expression was detected in SKOV-3 cells (Fig. 2*B* and *C*). Therefore, SKOV-3 cells were used as negative controls in our study. We generated tumor xenografts on BALB/c mice with either Caov-3 or SKOV-3 cells. Western blot analysis showed that FSHR was expressed only in Caov-3 xenografts and reproductive organs (uterus and ovary). No FSHR expression was detected in the heart, liver, spleen, lung, and kidney of BALB/c mice or SKOV-3 xenograft (Fig. 2*D*). These results confirmed that the distribution of FSHR was limited to specific organs and tissue. Therefore, a FSHR-targeted therapeutic strategy could be used to introduce drugs specifically to those related organs.

**Peptide FSH β 33-53 specifically bonded to FSHR-expressing human ovarian cancer cells.** To prove that peptide FSH β 33-53 could bind specifically to ovarian cancer cells that are expressing FSHR, FITC-labeled FSH β 33-53 peptide was incubated with either SKOV-3 or Caov-3 cells followed by fluorescence microscopy and flow cytometry examination. This peptide could bind to the FSHR-positive Caov-3 cells, but hardly to FSHR-negative SKOV-3 cells, even with extended incubation times (120 minutes) or high concentration (80 μmol/L; Fig. 3*A* and *B*). The increased fluorescence intensity in Caov-3 cells correlated with both the incubation time and the peptide concentration. By flow cytometry, mean fluorescence intensity of Caov-3 cells was significantly higher

Published OnlineFirst July 28, 2009; DOI: 10.1158/0008-5472.CAN-08-4721



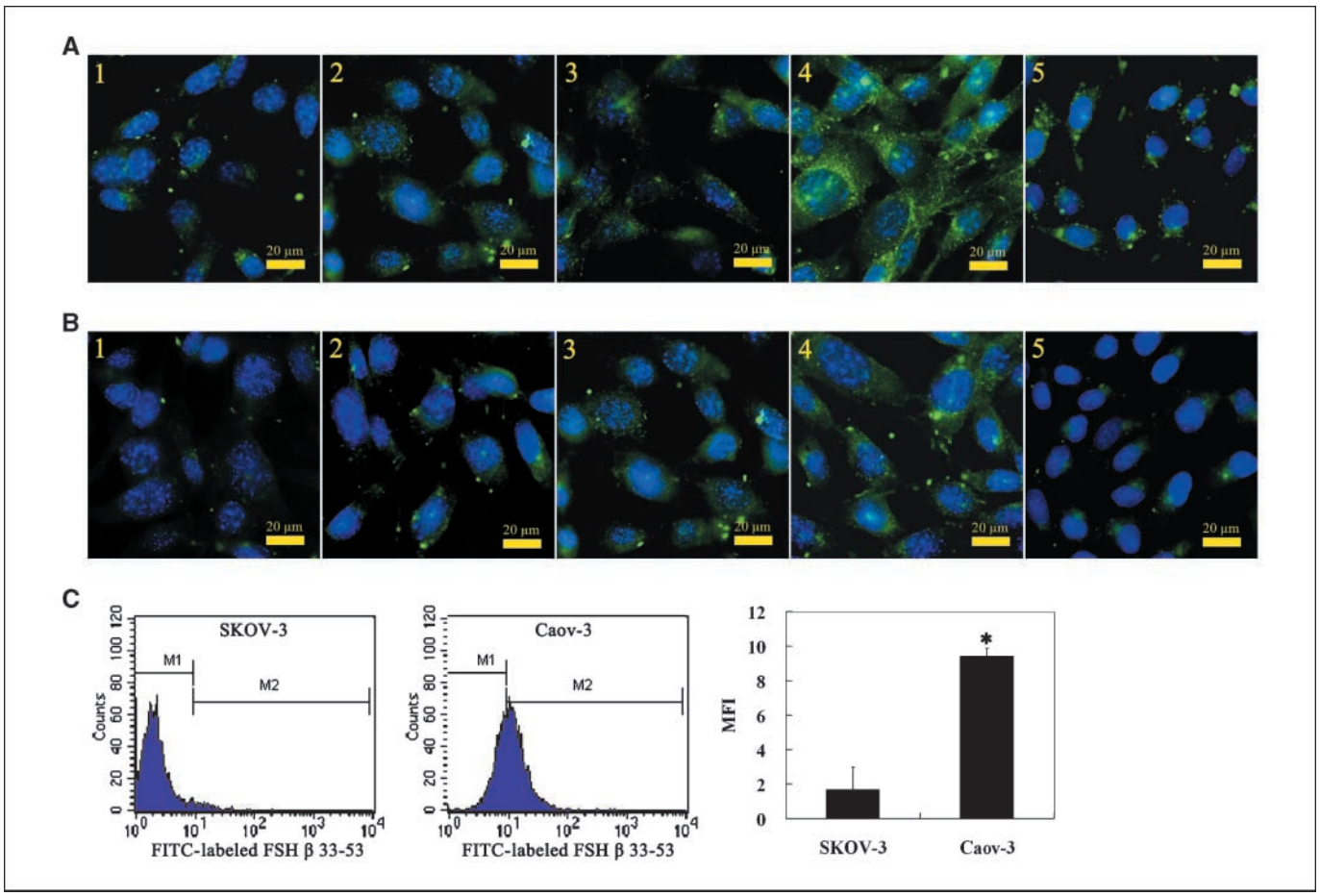


**Figure 3.** FITC-labeled FSH β 33-53 uptake by human ovarian cancer cells. *Bar,* 20 μm. *A,* FSH β 33-53 uptake within 60 min with different concentrations. *1* to *4,* Caov-3 cells treated with 10, 20, 40, and 80 μmol/L of peptide, respectively; *5,* SKOV-3 cells treated with 80 μmol/L of peptide. *B,* cells were incubated with 20 μmol/L of FSH β 33-53 for different times. *1* to *4,* Caov-3 cells treated for 15, 30, 60, and 120 min, respectively; *5,* SKOV-3 cells treated for 120 min. *C,* flow cytometry examination on Caov-3 and SKOV-3 cells treated with 20 μmol/L of FITC-labeled FSH β 33-53 for 60 min.

than SKOV-3 cells after 60 minutes of incubation with 20 μmol/L of FITC-labeled FSH β 33-53 peptide (9.443 ± 0.438 versus 1.677 ± 1.304; $P < 0.05$; Fig. 3*C*).

**FSH β 33-53 enables coumarin 6–loaded nanoparticles to specifically target Caov-3 cells.** As FSH β 33-53 peptide can bind to FSHR-expressing cells specifically, we then tested whether it can still bind to FSHR when conjugated to nanoparticles. To evaluate the uptake of nanoparticles, coumarin 6 was also incorporated into nanoparticles as a fluorescent indicator. The amount of FSH33-NP uptake in FSHR-positive Caov-3 cells was much higher than FSHR-negative SKOV-3 cells under the same conditions (Fig. 4*A*). Flow cytometry showed that there was no significant difference for the mean fluorescence intensities of SKOV-3 cells exposed to either FSH33-NP or nanoparticles alone. However, the mean fluorescence intensity of Caov-3 cells exposed to FSH33-NP was significantly higher than those exposed to naked nanoparticles (6.397 ± 0.287 versus 1.180 ± 1.021; $P < 0.05$). This amount of uptake in FSH33-NP increased with incubation time and FSH33-NP concentration (Fig. 4*B* and *C*). We also noticed that the uptake amount of coumarin 6–loaded FSH33-NP was much higher than that of coumarin 6–conjugated nanoparticles in Caov-3 cells (6.397 ± 0.287 versus 2.477 ± 0.428; $P < 0.05$; Fig. 4*D*), whereas the difference in the amount of nanoparticle uptake was not significant between Caov-3 and SKOV-3 cells. These data strongly suggested that FSH β 33-53 on the surface of nanoparticles could not only drive specific targeting at those cells expressing FSHR but also facilitate the uptake of drugs carried by nanoparticles into those cells.

**Effect of FSH33-NP-PTX on human ovarian cancer cells.** Next, we tested whether FSH33-NP could also mediate PTX delivery to those cells. PTX is a chemotherapeutic drug often used in patients with ovarian cancer, but it has very strong side effects due to nonspecific uptake by other organs and tissues. Therefore, more specific drug delivery would be desirable for PTX. We coupled PTX with FSH33-NP and first tested its antitumor effect *in vitro*. PTX, NP-PTX, or FSH33-NP-PTX was added to human ovarian cancer cells. The MTT assay showed that the proliferation of Caov-3 cells was inhibited in a concentration-dependent manner with $IC_{50}$s of 0.105, 0.284, and 1.198 μmol/L for FSH33-NP-PTX, NP-PTX, and PTX, respectively. Incorporation of PTX to nanoparticles decreased $IC_{50}$ by four times, and FSH peptide incorporation decreased $IC_{50}$ by another 2.7 times. The inhibition rate of FSH33-NP-PTX was ~15% higher than NP-PTX at 0.1 μmol/L in Caov-3 cells (Fig. 5*A*), whereas FSH33-NP-PTX was approximately twice more effective than NP-PTX with a shorter incubation time (<24 hours; Fig. 5*B*). Although nanoparticles coupled with PTX could already help PTX uptake by cells, as NP-PTX is more effective than

Published OnlineFirst July 28, 2009; DOI: 10.1158/0008-5472.CAN-08-4721



PTX alone, NP-PTX is still a nonspecific drug and it could possibly cause similar side effects when used in patients. On the other hand, FSH33-NP-PTX showed higher specificity to FSHR-expressing cells. As shown in Fig. 5*C* and *D*, FSH33-NP-PTX exhibited stronger proliferation inhibition effects on Caov-3 and ES-2 cells than OVCAR-3 cells, which have a lower FSHR expression level. This significant inhibitive effect was not observed in OSE cells or FSHR nonexpressing cells SKOV-3. Due to its higher specificity,

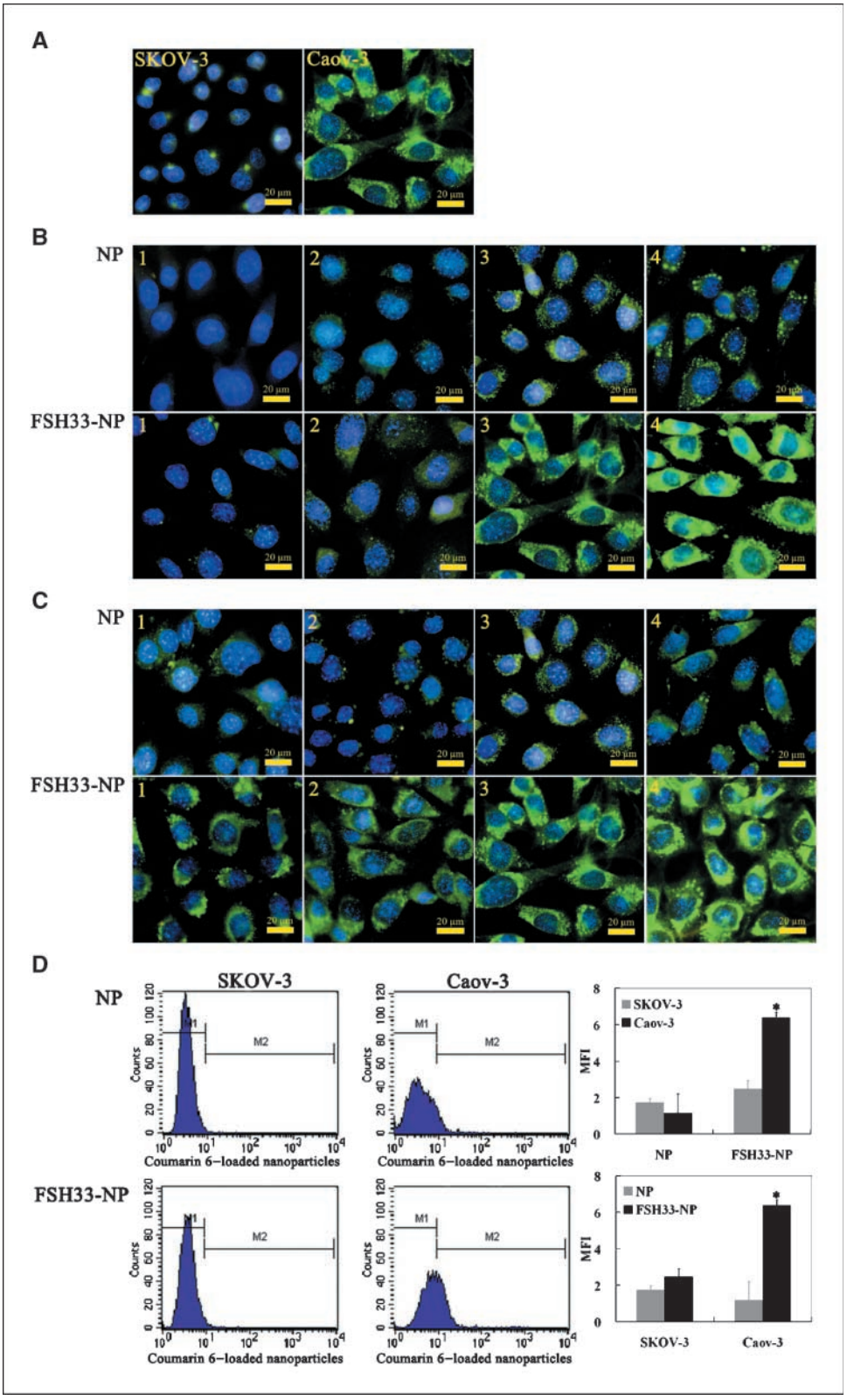


**Figure 4.** Specific uptake of coumarin 6–loaded FSH33-NP in FSHR-expressing Caov-3 cells. *Bar,* 20 μm. *A,* uptake of coumarin 6–loaded FSH33-NP in SKOV-3 or Caov-3 cells. Cells were incubated with 10 μg/mL nanoparticles for 60 min. Caov-3 cells were used in *B* and *C*. *B,* uptake of coumarin 6–loaded nanoparticles at different concentrations. *1* to *4,* cells incubated for 60 min with 0.1, 1, 10, and 100 μg/mL of nanoparticles, respectively. *C,* uptake of coumarin 6–loaded nanoparticles by incubating time. *1* to *4,* cells incubated with 10 μg/mL of nanoparticles for 15, 30, 60, and 120 min, respectively. *D,* uptake of coumarin 6–loaded nanoparticles (10 μg/mL nanoparticles for 60 min) in different cells by flow cytometry.

Published OnlineFirst July 28, 2009; DOI: 10.1158/0008-5472.CAN-08-4721



FSH33-NP-PTX was much more effective at lower concentrations and shorter incubation times. Taken together, our data suggested that FSH β 33-53 peptide–coupled NP-PTX could target FSHR-expressing cells more specifically and efficiently *in vitro*.

**FSH33-NP-PTX treatment for human ovarian carcinoma.** Next, we tested the antitumor effects of FSH33-NP-PTX *in vivo*. BALB/c mice bearing human ovarian cancer Caov-3 xenografts were administrated i.v. with either saline solution alone or saline with commercial PTX, NP-PTX, or FSH33-NP-PTX every 3 days for five consecutive injections. The concentration of the injected drugs was 6 mg/kg body weight, which was about half of the dose of PTX normally used in mice (31). The final tumor size of treated mice was notably reduced, especially for mice treated with FSH33-NP-PTX (Fig. 6*A*), and the tumor growth curve showed that tumor growth was delayed most prominently in the group treated with FSH33-NP-PTX (Fig. 6*B*). The final average volume and weight of tumor nodules in the FSH33-NP-PTX group were 0.29 ± 0.08 $cm^3$ and 0.33 ± 0.13 g, respectively, which were significantly smaller than the other three groups (Supplementary Table S3; Fig. 6*C* and *D*). The inhibitive rates calculated based on tumor volume and weight were 69.95% and 68.37% in the FSH33-NP-PTX group, about 2 times higher than those in the NP-PTX group and 3.5 times higher than those in the commercial PTX group. During the whole study, no obvious side effects to the mice were found. At the study end point, there were no significant differences in the average body weights between the four groups, and the pathologic staining of liver, spleen, and kidney showed no obvious differences in all groups (data not shown). These data indicated that nanoparticulate carriers and peptide FSH β 33-53 could facilitate the enrichment of drugs in tumor tissues so that the efficacy of drugs could be improved with a smaller dose.

## Discussion

In this study, we developed a novel active targeted therapeutic system, FSH33-NP, and showed its potential as a promising drug delivery strategy. FSH and its receptor have been implicated to play critical roles in the development of ovarian cancer (32–36). We found that 70.83% of human primary ovarian carcinoma specimens expressed FSHR, and FSHR expression was detected only in reproductive organs in BALB/c mice. Therefore, it is practicable to use FSHR as the specific target site against ovarian carcinoma with antagonisms of the receptor. Compared with commonly used monoclonal antibodies, peptides are smaller, easier to prepare, and have lower immunogenicity (3). Therefore, peptide FSH β 33-53 was chosen as a target-specific ligand due to its high affinity to FSHR. This peptide was covalently attached to PEG-PLA nanoparticles.

The covalent attachment of FSH β 33-53 peptide and nanoparticles was achieved by means of the sulfhydryl groups of FSH β 33-53 peptides and the maleimide groups on the surface of nanoparticles. XPS was performed to investigate whether the covalent attachment was successful based on the amount of surface nitrogen (13). XPS is a surface-sensitive chemical analysis technique that measures the elemental composition, empirical formula, chemical state, and electronic state of the elements of a material. The kinetic energy and number of electrons that escape from the upper 1 to 10 nm of the material can be measured. The

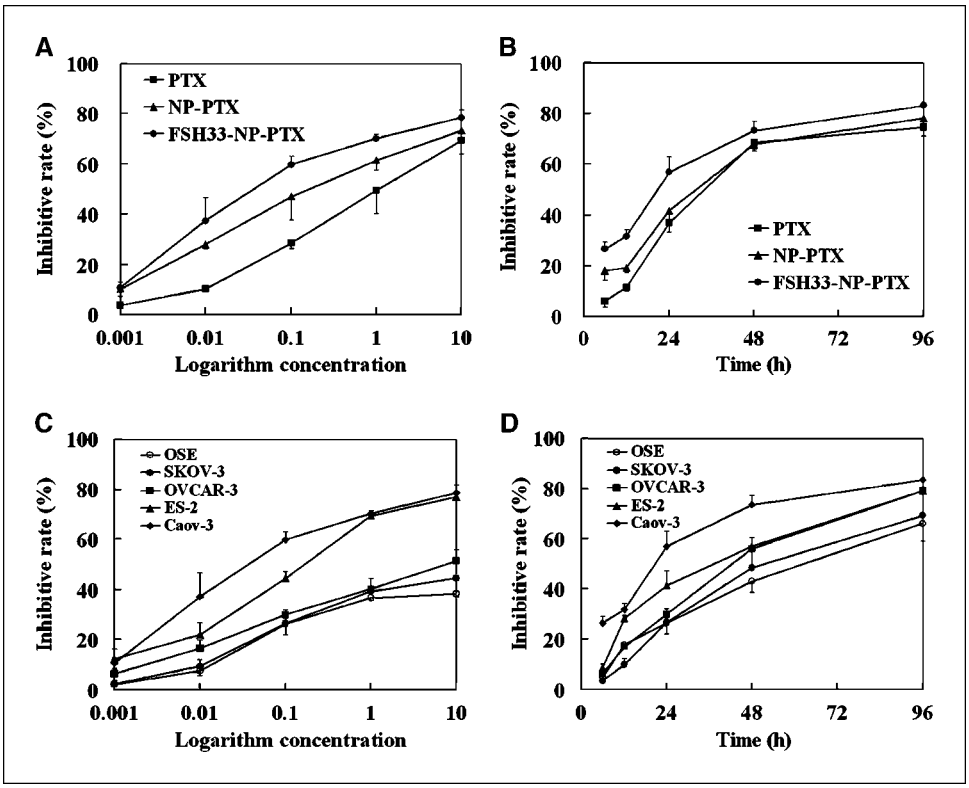


**Figure 5.** Inhibitive effects of FSH33-NP-PTX by MTT assay. *A,* inhibitive rate-concentration curve of different PTX samples on Caov-3 cells after 24-h incubation. The $IC_{50}$s of FSH33-NP-PTX, NP-PTX, and PTX were 0.105, 0.284, and 1.198 μmol/L. *B,* inhibitive rate-time curve of Caov-3 cells incubated with 0.1 μmol/L of different PTX samples. *C,* inhibitive rate-concentration curve of different cells with FSH33-NP-PTX. Cells were incubated for 24 h. *D,* inhibitive rate-time curve of different cells with 0.1 μmol/L of FSH33-NP-PTX.

Published OnlineFirst July 28, 2009; DOI: 10.1158/0008-5472.CAN-08-4721



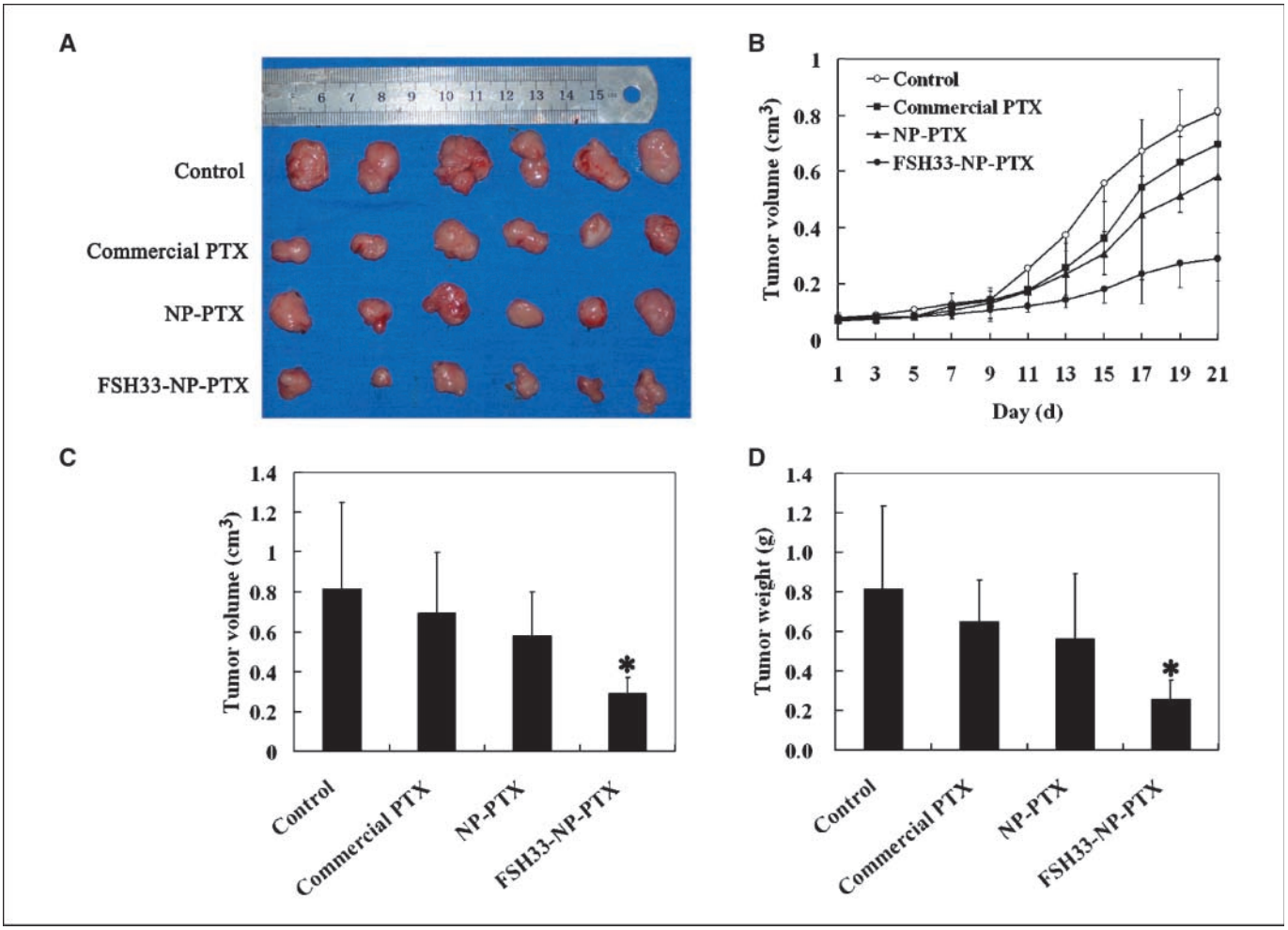


**Figure 6.** Antitumor effects of FSH33-NP-PTX on BALB/c mice bearing human ovarian carcinoma. Four groups were administrated i.v. with either saline, commercial PTX, NP-PTX, or FSH33-NP-PTX. The injection was repeated every 3 d for five consecutive injections (days 1, 4, 7, 10, and 13). At day 21, mice were sacrificed. *A,* tumor xenografts of mice at the study end point. *B,* tumor growth curve during the whole experiment. Tumor size was determined as described in Materials and Methods. *C,* tumor volume at the study end point. *D,* tumor weight at the study end point.

detection limit of XPS is 0.1% (30). In this study, the N1s envelope was only detected in FSH33-NP, which indicated that the detected N1s signal of FSH33-NP ascribed to FSH β 33-53 peptides on the surface of nanoparticles.

In our study, FSH33-NP was efficiently uptaken by FSHR-positive Caov-3 cells (Fig. 4), as FSH β 33-53 on the surface of nanoparticles could be specifically recognized by FSHR (Fig. 3). The mechanism might be receptor-mediated endocytosis (37, 38). This kind of endocytosis results in efficient internalization of ligand-modified carriers in receptor-expressing cells (39–41). Our results are similar to other studies showing receptor-targeted therapy for ovarian cancer (42–44). A common chemotherapeutic drug in ovarian cancer, PTX, was incorporated into nanoparticle carriers. The antitumor efficiency of FSH33-NP-PTX was determined both *in vitro* and *in vivo*. On a tumor xenograft model, the antitumor effect of FSH33-NP-PTX was significantly stronger than commercial PTX or NP-PTX. The tumor-inhibitive rate of FSH33-NP-PTX almost reached 70% and this was about 2 times higher than NP-PTX and 3.5 times higher than commercial PTX. Our data not only confirmed that nanoparticulate carriers could enhance the PTX effect (45) but also suggested that FSH β 33-53 peptide could further enhance the antitumor effect. However, the definite mechanisms of how FSH β 33-53 facilitated the delivery of nanoparticles still need further investigation.

Another great thing about our method is that a smaller dose of PTX (6 mg/kg body weight) was given to those mice. Consequently, no obvious side effects were observed (data no shown). This would be of great help to cancer patients during chemotherapy as it could reduce the pain they normally experience. Currently, most patients with ovarian cancer have to go through surgery to remove both ovaries and uterus followed by chemotherapy. If the future diagnosis for ovarian cancer could be done in earlier stages when the cancer cells have not migrated to other organs, our new drug delivery system could even be used before surgery to target ovarian carcinoma on-site first.

Taken together, this study showed that FSH β 33-53 peptide had the potential to facilitate the access of drugs carried by nanoparticles with a high selectivity to ovarian tumor tissues expressing FSHR. This novel FSH33-NP delivery system could not only enhance the antitumor effect of chemotherapeutic drugs but also minimize side effects in unrelated normal organs, and this delivery system could also be used for therapeutic drugs other than PTX to fight against ovarian cancer. Further studies will be needed to illuminate these mechanisms.

Published OnlineFirst July 28, 2009; DOI: 10.1158/0008-5472.CAN-08-4721



## Disclosure of Potential Conflicts of Interest

No potential conflicts of interest were disclosed.

## Acknowledgments

Received 12/16/08; revised 4/26/09; accepted 6/5/09; published OnlineFirst 7/28/09.

**Grant support:** Research Scholar Fund of Shanghai Medical School, Fudan University; Shanghai Leading Academic Discipline Project, Project no. B117; National High-tech R&D Program (863 Program), Project no. 2006AA02Z342; Shanghai Science Committee emphasis project, Project no. 044119601; and Scientific Research Program of Nanometer of Shanghai Science Committee, Project no. 0852nm04500.

The costs of publication of this article were defrayed in part by the payment of page charges. This article must therefore be hereby marked *advertisement* in accordance with 18 U.S.C. Section 1734 solely to indicate this fact.

We thank Prof. Fu-you Li (Laboratory of Advanced Materials, Fudan University), Prof. Wei-yue Lu (Department of Pharmaceutics, School of Pharmacy, Fudan University), and Prof. Da-jin Li and Dr. Liang-qing Yao (Obstetrics and Gynecology Hospital, Fudan University) for their valuable guidance.

## References

1. Schally AV, Nagy A. Chemotherapy targeted to cancers through tumoral hormone receptors. Trends Endocrinol Metab 2004;15:300–10.
2. Brigger I, Dubernet C, Couvreur P. Nanoparticles in cancer therapy and diagnosis. Adv Drug Deliv Rev 2002; 54:631–51.
3. Kumar P, Wu H, McBride JL, et al. Transvascular delivery of small interfering RNA to the central nervous system. Nature 2007;448:39–43.
4. Cirstoiu-Hapca A, Bossy-Nobs L, Buchegger F, Gurny R, Delie F. Differential tumor cell targeting of anti-HER2 (Herceptin) and anti-CD20 (Mabthera) coupled nanoparticles. Int J Pharm 2007;331:190–6.
5. Nagy A, Schally AV. Targeting cytotoxic conjugates of somatostatin, luteinizing hormone-releasing hormone and bombesin to cancers expressing their receptors: a "smarter" chemotherapy. Curr Pharm Des 2005;11: 1167–80.
6. Koo OM, Rubinstein I, Onyuksel H. Role of nanotechnology in targeted drug delivery and imaging: a concise review. Nanomedicine 2005;1:193–212.
7. Panyam J, Labhasetwar V. Biodegradable nanoparticles for drug and gene delivery to cells and tissue. Adv Drug Deliv Rev 2003;55:329–47.
8. Kim JS, Rieter WJ, Taylor KM, An H, Lin W, Lin W. Self-assembled hybrid nanoparticles for cancer-specific multimodal imaging. J Am Chem Soc 2007;129:8962–3.
9. Gref R, Minamitake Y, Peracchia MT, Trubetskoy V, Torchilin V, Langer R. Biodegradable long-circulating polymeric nanospheres. Science 1994;263:1600–3.
10. Bazile D, Prud'homme C, Bassoullet MT, Marlard M, Spenlehauer G, Veillard M. Stealth Me.PEG-PLA nanoparticles avoid uptake by the mononuclear phagocytes system. J Pharm Sci 1995;84:493–8.
11. Olivier JC, Huertas R, Lee HJ, Calon F, Pardridge WM. Synthesis of pegylated immunonanoparticles. Pharm Res 2002;19:1137–43.
12. Vila A, Sanchez A, Tobio M, Calvo P, Alonso MJ. Design of biodegradable particles for protein delivery. J Control Release 2002;78:15–24.
13. Lu W, Zhang Y, Tan YZ, Hu KL, Jiang XG, Fu SK. Cationic albumin-conjugated pegylated nanoparticles as novel drug carrier for brain delivery. J Control Release 2005;107:428–48.
14. Lu W, Tan YZ, Hu KL, Jiang XG. Cationic albumin conjugated pegylated nanoparticle with its transcytosis ability and little toxicity against blood-brain barrier. Int J Pharm 2005;295:247–60.
15. Nakano R, Kitayama S, Yamoto M, Shima K, Ooshima A. Localization of gonadotropin binding sites in human ovarian neoplasms. Am J Obstet Gynecol 1989;161:905–10.
16. Parrott JA, Doraiswamy V, Kim G, Mosher R, Skinner MK. Expression and actions of both the follicle stimulating hormone receptor and the luteinizing hormone receptor in normal ovarian surface epithelium and ovarian cancer. Mol Cell Endocrinol 2001;172:213–22.
17. Syed V, Ulinski G, Mok SC, Yiu GK, Ho SM. Expression of gonadotropin receptor and growth responses to key reproductive hormones in normal and malignant human ovarian surface epithelial cells. Cancer Res 2001;61:6768–76.
18. Al-Timimi A, Buckley CH, Fox H. An immunohistochemical study of the incidence and significance of human gonadotrophin and prolactin binding sites in normal and neoplastic human ovarian tissue. Br J Cancer 1986;53:321–9.
19. Zheng W, Lu JJ, Luo F, et al. Ovarian epithelial tumor growth promotion by follicle-stimulating hormone and inhibition of the effect by luteinizing hormone. Gynecol Oncol 2000;76:80–8.
20. Minegishi T, Kameda T, Hirakawa T, Abe K, Tano M, Ibuki Y. Expression of gonadotropin and activin receptor messenger ribonucleic acid in human ovarian epithelial neoplasms. Clin Cancer Res 2000;6:2764–70.
21. Wang J, Lin L, Parkash V, Schwartz PE, Lauchlan SC, Zheng W. Quantitative analysis of follicle-stimulating hormone receptor in ovarian epithelial tumors: a novel approach to explain the field effect of ovarian cancer development in secondary mullerian systems. Int J Cancer 2003;103:328–34.
22. Zheng W, Magid MS, Kramer EE, Chen YT. Follicle-stimulating hormone receptor is expressed in human ovarian surface epithelium and fallopian tube. Am J Pathol 1996;148:47–53.
23. Santa-Coloma TA, Grasso P, Reichert LE, Jr. Synthetic human follicle-stimulating hormone-β-(1-15) peptide-amide binds $Ca^{2+}$ and possesses sequence similarity to calcium binding sites of calmodulin. Endocrinology 1992;130:1103–7.
24. Agris PF, Guenther RH, Sierzputowska-Gracz H, et al. Solution structure of a synthetic peptide corresponding to a receptor binding region of FSH (hFSH-β 33-53). J Protein Chem 1992;11:495–507.
25. Grasso P, Santa-Coloma TA, Reichert LE, Jr. Synthetic peptides corresponding to human follicle-stimulating hormone (hFSH)-β-(1-15) and hFSH-β-(51-65) induce uptake of 45Ca++ by liposomes: evidence for calcium-conducting transmembrane channel formation. Endocrinology 1991;128:2745–51.
26. Santa Coloma TA, Reichert LE, Jr. Identification of a follicle-stimulating hormone receptor-binding region in hFSH-β-(81-95) using synthetic peptides. J Biol Chem 1990;265:5037–42.
27. Zhang Y, Zhang Q, Zha L, et al. Preparation, characterization and application of pyrene-loaded methoxy poly(ethylene glycol)-poly(lactic acid) copolymer nanoparticles. Colloid Polym Sci 2004;282:1323–8.
28. Tobio M, Gref R, Sanchez A, Langer R, Alonso MJ. Stealth PLA-PEG nanoparticles as protein carriers for nasal administration. Pharm Res 1998;15:270–5.
29. Quellec P, Gref R, Dellacherie E, Sommer F, Tran MD, Alonso MJ. Protein encapsulation within poly(ethylene glycol)-coated nanospheres. II. Controlled release properties. J Biomed Mater Res 1999;47:388–95.
30. Dong Y, Feng SS. Methoxy poly(ethylene glycol)-poly(lactide) (MPEG-PLA) nanoparticles for controlled delivery of anticancer drugs. Biomaterials 2004;25:2843–9.
31. Rosano L, Spinella F, Salani D, et al. Therapeutic targeting of the endothelin A receptor in human ovarian carcinoma. Cancer Res 2003;63:2447–53.
32. Landen CN, Jr., Birrer MJ, Sood AK. Early events in the pathogenesis of epithelial ovarian cancer. J Clin Oncol 2008;26:995–1005.
33. Konishi I. Gonadotropins and ovarian carcinogenesis: a new era of basic research and its clinical implications. Int J Gynecol Cancer 2006;16:16–22.
34. Edmondson RJ, Monaghan JM, Davies BR. Gonadotropins mediate DNA synthesis and protection from spontaneous cell death in human ovarian surface epithelium. Int J Gynecol Cancer 2006;16:171–7.
35. Li Y, Ganta S, Cheng C, Craig R, Ganta RR, Freeman LC. FSH stimulates ovarian cancer cell growth by action on growth factor variant receptor. Mol Cell Endocrinol 2007;267:26–37.
36. Choi JH, Choi KC, Auersperg N, Leung PC. Gonadotropins activate proteolysis and increase invasion through protein kinase A and phosphatidylinositol 3-kinase pathways in human epithelial ovarian cancer cells. Cancer Res 2006;66:3912–20.
37. Moyle WR, Lin W, Myers RV, Cao D, Kerrigan JE, Bernard MP. Models of glycoprotein hormone receptor interaction. Endocrine 2005;26:189–205.
38. Walther TC, Brickner JH, Aguilar PS, Bernales S, Pantoja C, Walter P. Eisosomes mark static sites of endocytosis. Nature 2006;439:998–1003.
39. Henriques ST, Melo MN, Castanho MA. Cell-penetrating peptides and antimicrobial peptides: how different are they? Biochem J 2006;399:1–7.
40. Westphalen S, Kotulla G, Kaiser F, et al. Receptor mediated antiproliferative effects of the cytotoxic LHRH agonist AN-152 in human ovarian and endometrial cancer cell lines. Int J Oncol 2000;17:1063–9.
41. Arencibia JM, Schally AV, Halmos G, Nagy A, Kiaris H. *In vitro* targeting of a cytotoxic analog of luteinizing hormone-releasing hormone AN-207 to ES-2 human ovarian cancer cells as demonstrated by microsatellite analyses. Anticancer Drugs 2001;12:71–8.
42. Kalli KR, Oberg AL, Keeney GL, et al. Folate receptor α as a tumor target in epithelial ovarian cancer. Gynecol Oncol 2008;108:619–26.
43. Dijkgraaf I, Kruijtzer JA, Frielink C, et al. αvβ3 integrin-targeting of intraperitoneally growing tumors with a radiolabeled RGD peptide. Int J Cancer 2007;120: 605–10.
44. Thompson S, Dessi J, Self CH. The construction and *in vitro* testing of photo-activatable cancer targeting folated anti-CD3 conjugates. Biochem Biophys Res Commun 2008;366:526–31.
45. Lu H, Li B, Kang Y, et al. Paclitaxel nanoparticle inhibits growth of ovarian cancer xenografts and enhances lymphatic targeting. Cancer Chemother Pharmacol 2007;59:175–81.

Cancer Research
The Journal of Cancer Research (1916–1930) | The American Journal of Cancer (1931–1940)

AACR American Association for Cancer Research

# Follicle-Stimulating Hormone Peptide Can Facilitate Paclitaxel Nanoparticles to Target Ovarian Carcinoma *In vivo*

Xiao-yan Zhang, Jun Chen, Yu-fang Zheng, et al.

*Cancer Res* 2009;69:6506-6514. Published OnlineFirst July 28, 2009.